Supplementary Information

Synthesis and Elucidation of Local Structure in Phase-Controlled Colloidal Tin Phosphide Nanocrystals from Aminophosphines

Authors: Ingrid J. Paredes[1], Amani M. Ebrahim[2], Rito Yanagi[1,3,4], Anna M. Plonka[2], Shuzhen Chen[1], Hanlu Xia[1], Scott Lee[1], Mersal Khwaja[1], Haripriya Kannan[1], Ajay Singh[5], Sooyeon Hwang[6], Anatoly I. Frenkel[2,7], Ayaskanta Sahu[1]

Affiliations:

[1]Department of Chemical and Biomolecular Engineering, New York University Tandon School of Engineering, 6 Metrotech Center, Brooklyn, New York, 11201, United States

[2]Department of Materials Science and Chemical Engineering, Stony Brook University, Stony Brook, New York 11794, United States

[3]Department of Chemical and Environmental Engineering, Yale University, New Haven, Connecticut, 06520, United States.

[4]Energy Sciences Institute, Yale University, 810 West Campus Drive, West Haven, Connecticut, 06516, United States

[5]Center for Integrated Nanotechnologies, Material Physics and Applications Division, Los Alamos National Laboratory, Los Alamos, New Mexico 87545, United States

[6]Center for Functional Nanomaterials, Brookhaven National Laboratory, Upton, New York 11973, United States

[7]Chemistry Division, Brookhaven National Laboratory, Upton, New York 11973, United States

*Correspondence to: asahu@nyu.edu, anatoly.frenkel@stonybrook.edu

1. Characterization

1.1 X-ray Diffraction (XRD)

XRD characterization was performed using a Bruker AXS D8 DISCOVER GADDS Microdiffractometer with Cu Kα radiation (λ = 0.154 nm). Samples were prepared by drop casting a concentrated solution of nanoparticles from toluene onto a 1 cm x 1 cm <100> silicon substrate inside of a nitrogen filled glovebox. XRD scans were collected using an incident angle of ω = 18°. XRD data was processed using GSAS-II software.[1]

1.1.2 Scherrer Analysis

The crystal grain size, τ, is given by

$$\tau = \frac{K\lambda}{\beta cos\theta}$$

where K is the dimensionless Scherrer constant, λ is the X-ray wavelength in nm, β is the line broadening (FWHM) and θ is the Bragg angle in radians. In our analysis, K = 0.9 and λ = 0.154 nm. β was approximated from a Gaussian fit of diffraction peaks. The final crystal grain size was obtained by taking an average estimation from several peaks. For Sn_4P_3 nanocrystals, using the characteristic peak at 2θ = 31°, a Gaussian fit provided β = 0.514°, providing a τ = 20.2 nm.

1.2 Transmission Electron Microscopy (TEM)

TEM samples were prepared on 300 mesh formvar/carbon grids (Ted Pella, FCF300-Cu-UA). Bright field TEM images were obtained using a Tecnai Spirit 120kV TEM. The particle size distribution of each sample was determined using the ImageJ software.[2] For high resolution TEM (HRTEM), samples were prepared by drop casting a dilute filtered solution of nanoparticles dispersed in hexanes onto a TEM grid. Images were taken using a FEI Titan Themis 200 kV TEM. Scanning transmission electron microscopy (STEM) images and energy dispersive X-ray (EDX)

measurements were acquired with a Hitachi HD2700C dedicated STEM with a probe Cs corrector at an accelerating voltage of 200 kV.

1.3 X-ray Photoelectron Spectroscopy (XPS)

XPS data was measured using a Versa Probe II XPS from Physical Electronics with Al Kα source operated at 50 W and 15 kV with an energy resolution of 700 meV and 200 μm spot size. Samples were prepared by drop casting a solution of nanoparticles onto a 1 cm x 1 cm glass slide (Thin Film Devices). The data was processed using MultiPak Data Reduction software, in which sample spectra were calibrated to the carbon spectrum.

1.4 X-ray Absorption Spectroscopy (XAS)

X-ray absorption measurements were conducted at the 7-BM (Quick Absorption and Scattering, QAS) beamline at NSLS-II. Samples were prepared by drop casting dispersions of nanoparticles from toluene, and drying them to make thick films onto pieces of Kapton. The Kapton pieces were then folded and sealed with Kapton tape under an inert nitrogen atmosphere prior to sample loading. Extended X-ray absorption fine structure (EXAFS) measurements at the Sn K-edge were performed in transmission mode using a Si (111) crystal monochromator detuned by 20%. Sn foil was used for calibration and alignment of all data in X-ray energy. The ionization chambers were filled with 90% Ar and 10% N_2.

EXAFS data was processed using the Demeter software package (Athena and Artemis).[3] The collected XAS spectra were aligned, merged, normalized, and background subtracted in Athena. The theoretical EXAFS spectra were then constructed using the FEFF6 code incorporated in Artemis. The fitting was performed in r-space using a Hanning window applied to the k^2- weighted data. The amplitude reduction factor (S_0^2) was obtained from fitting EXAFS data for the Sn foil collected at QAS fitted to Sn metal (ICSD-236667) and was determined to be 1.1 ± 0.2. Corrections

to the theoretical photoelectron energy (ΔE_0), the nearest coordination number (N), and the disorder term (σ^2) were varied during the fits.

2. Supplementary Figures and Tables

Table S1. Legend of Phases and Figures

Phase	Corresponding Figures
SnP	Figure 3, Figure 6, Figure 7, Figure 8a, Figure 8b
Sn_4P_3	Figure 4, Figure, Figure 7, Figure 8c, Figure 8d
Sn_3P_4	Figure 5, Figure 6, Figure 7, Figure 8e, Figure 8d, Figure S7

Table S2. List of the structure models used in the EXAFS fitting approach.

Model	Identifier	Structure and Space Group	Coordination Environment (Number)	Radial Distance (Å)
SnP	ICSD-16077	Tetragonal I 4 m m	Sn-P (3)	2.63
SnP	ICSD-69026	Trigonal P -3 m 1	Sn-P (2) Sn-P (1)	1.96 2.52
Sn_3P_4	Huang *et al.*[4]	Trigonal P 3 1 c	Sn-P (1) Sn-P (3)	2.48 2.52
Sn_3P_4	COD-4001104	Hexagonal R -3 m	Sn-P (12)	2.68
Sn_4P_3	ICSD-15014	Rhombohedral R -3 m H	Sn-P (3)	2.66
SnO	ICSD-16481	Tetragonal P 4 / n m m	Sn-O (1)	1.84

1

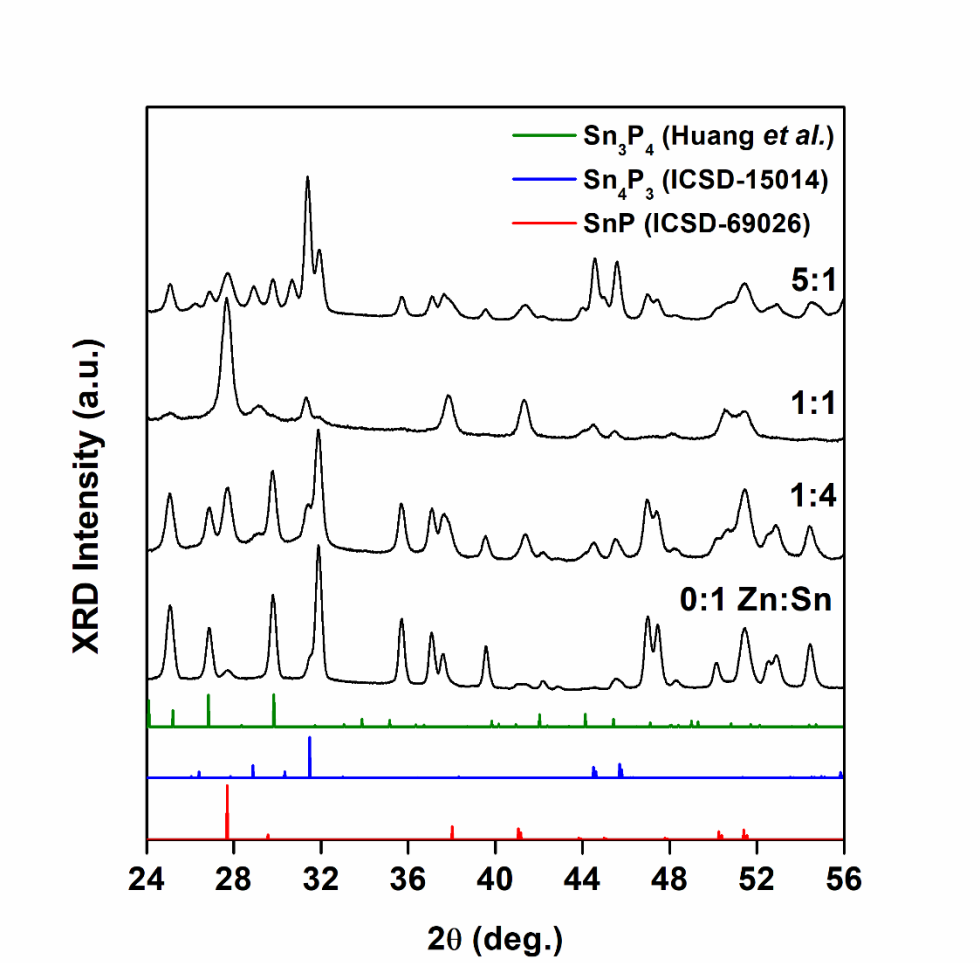

Figure S1. The effect of the ratio of zinc to tin on reaction products. X-ray diffraction data (XRD) for nanoparticles synthesized in the absence of $ZnCl_2$, a 1:4 ratio, a 1:1 ratio, and a 5:1 ratio of $ZnCl_2$:$SnCl_2$, are shown. All other reaction parameters were held constant across syntheses. Data are plotted against reference data for SnP (ICSD-69026), Sn_4P_3 (ICSD-15014), and Sn_3P_4 (Huang et al.[4]). At all ratios, we obtained phase-mixtures of various tin phosphides.

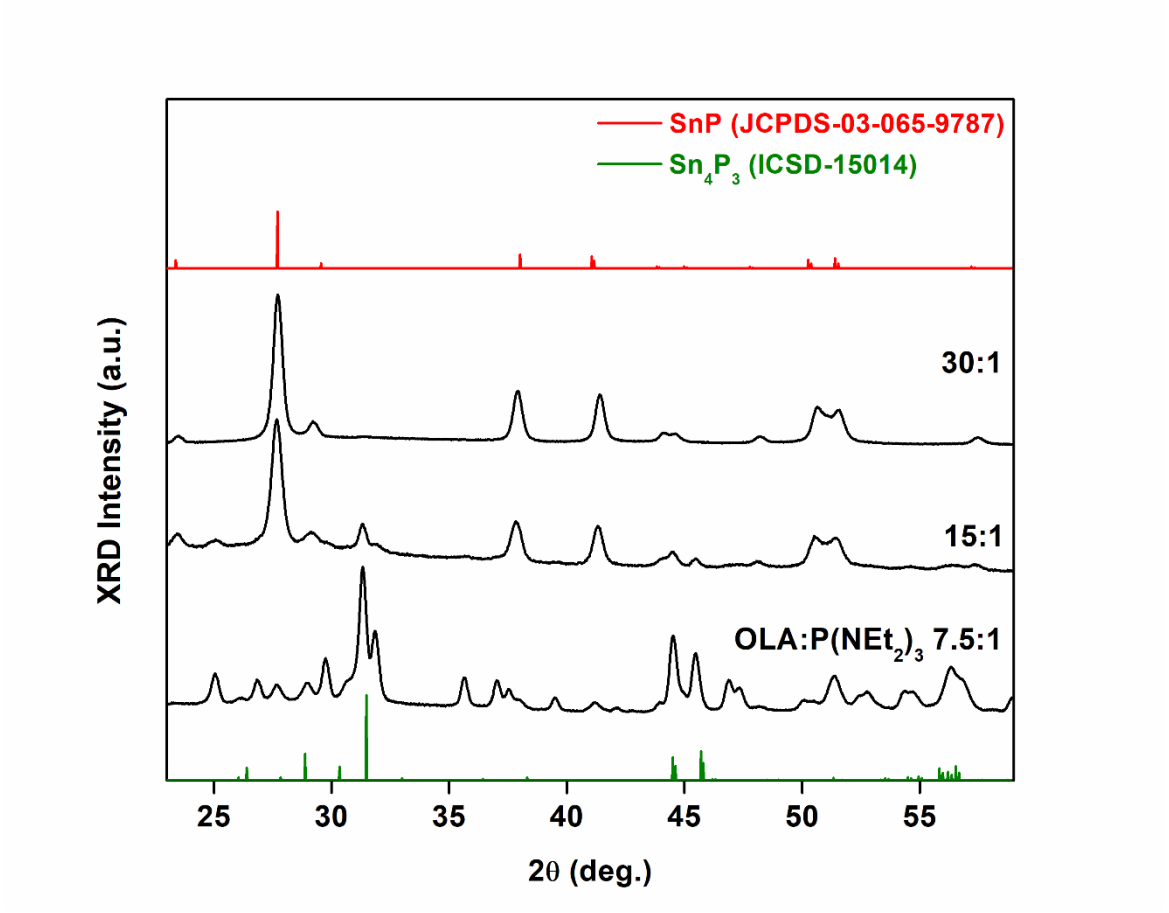

Figure S2. The effect of the amount of oleylamine (OLA) on reaction products. X-ray diffraction data (XRD) for nanoparticles synthesized in a 7.5:1, 15:1, and 30:1 ratio of OLA to trisdiethylaminophosphine $(PNEt_2)_3$, are shown. All other reaction parameters were held constant aross experiments. The data is plotted against reference data for SnP (JCPDS-69026) and Sn_4P_3 (ICSD-15014). Increasing the ratio of oleylamine to $P(NEt_2)_3$ drove the reaction pathway towards SnP. At the highest ratio of oleylamine to $P(NEt_2)_3$, we obtained a phase pure SnP.

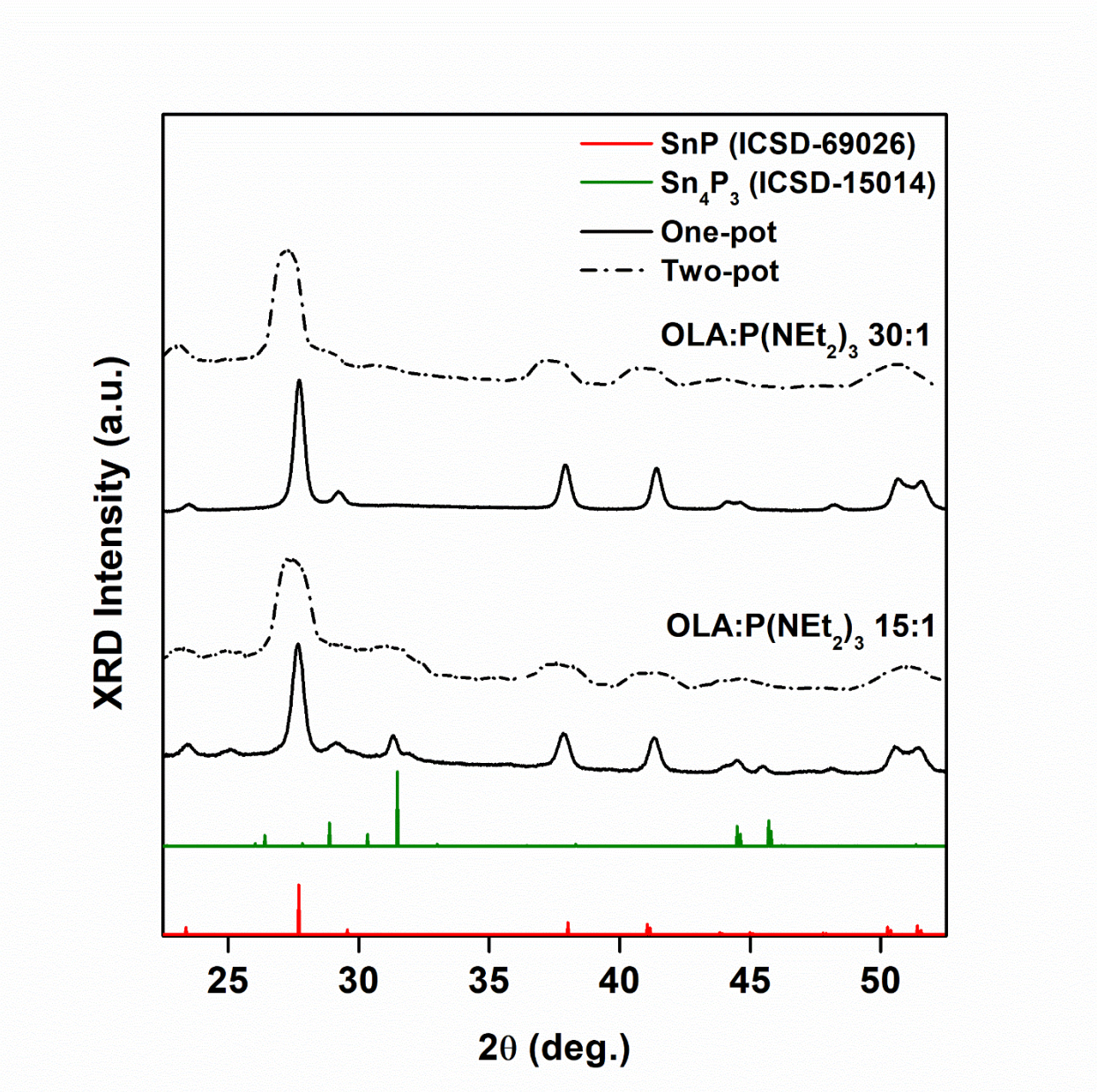

Figure S3. Phase data for tin phosphide nanocrystals grown under one-pot (solid) and two-pot (dashed) conditions. The data showed a similar trend regardless of method; increasing the ratio of oleylamine (OLA) to trisdiethylaminophosphine ($(PNEt_2)_3$) shifted the reaction towards phase-pure SnP nanocrystals.

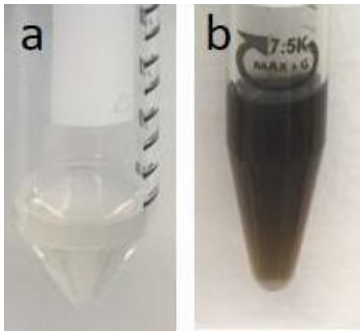

Figure S4. Dispersion of nanoparticles in toluene after filtration through 0.2 μm PTFE membrane from (**a**) synthesis without oleic acid, in which case particles aggregated and did not filter, and (**b**) synthesis with oleic acid, in which particles filtered.

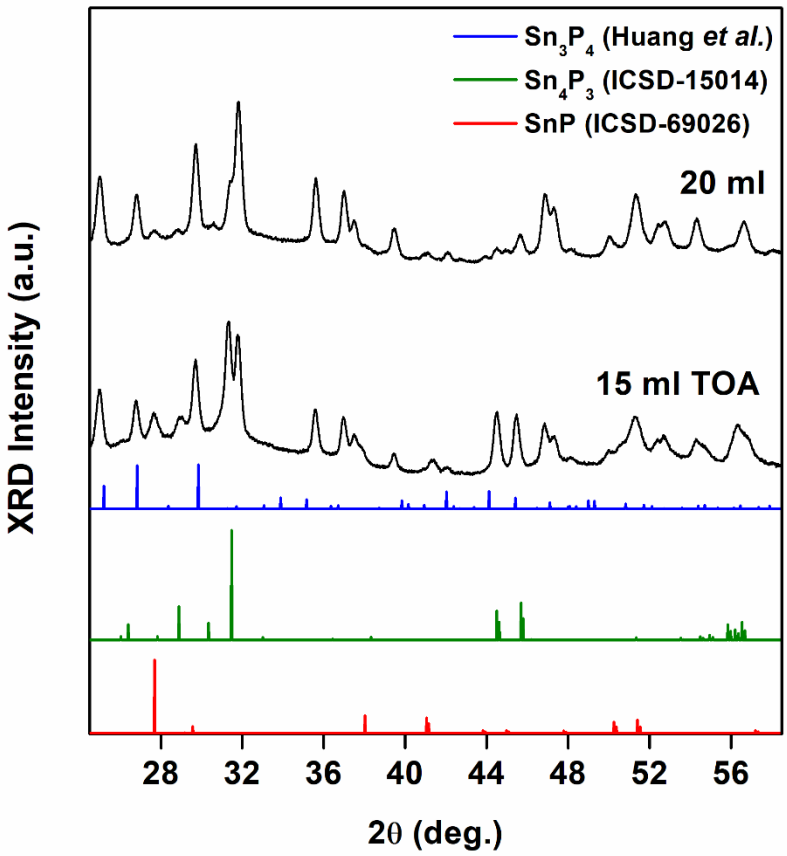

Figure S5. X-ray diffraction (XRD) data for tin phosphide nanocrystals grown in the presence of varying amounts of trioctylamine (TOA) (15 mL, 20 mL,) for 2 minutes at 250°C following injection of trisdiethylaminophosphine. ($P(NEt_2)_3$) for 2 minutes at 250°C. Data is plotted against reference data for Sn_4P_3 (ICSD-15014), SnP (ICSD-69026), and Sn_3P_4 (Huang *et al.*[4]).

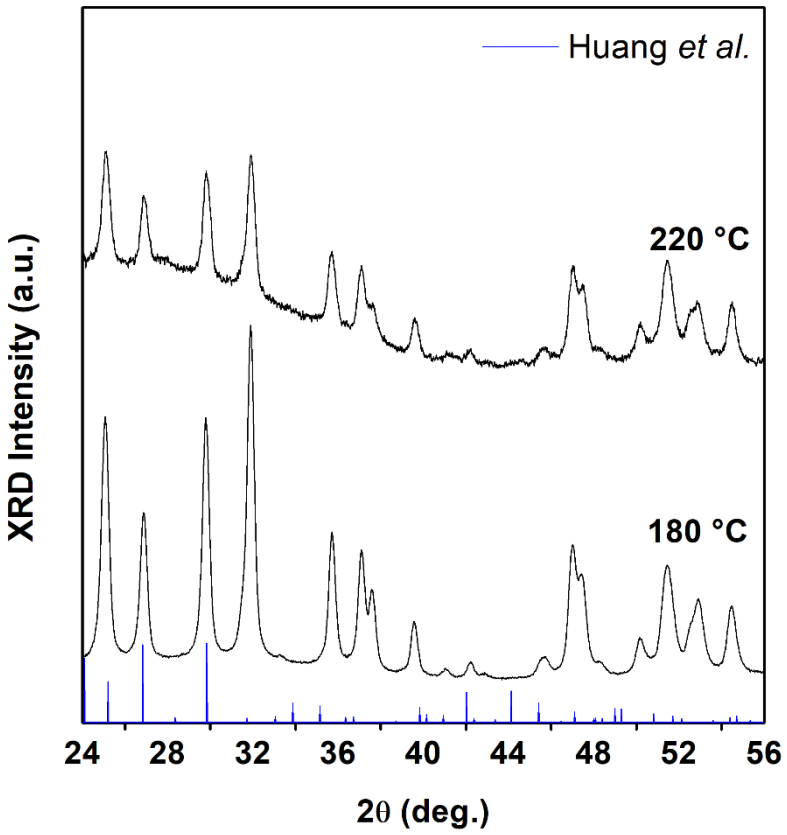

Figure S6. The effect of temperature on reaction products. X-ray diffraction (XRD) data for tin phosphide nanocrystals grown for 2 min at 250 °C following injection of trisdiethylaminophosphine $(PNEt_2)_3$ into 20 mL of oleylamine and equimolar amounts of $SnCl_2$ and $ZnCl_2$ at 180 °C and 220 °C. The data were comparable to a trigonal Sn_3P_4 structure predicted by Huang *et al*.

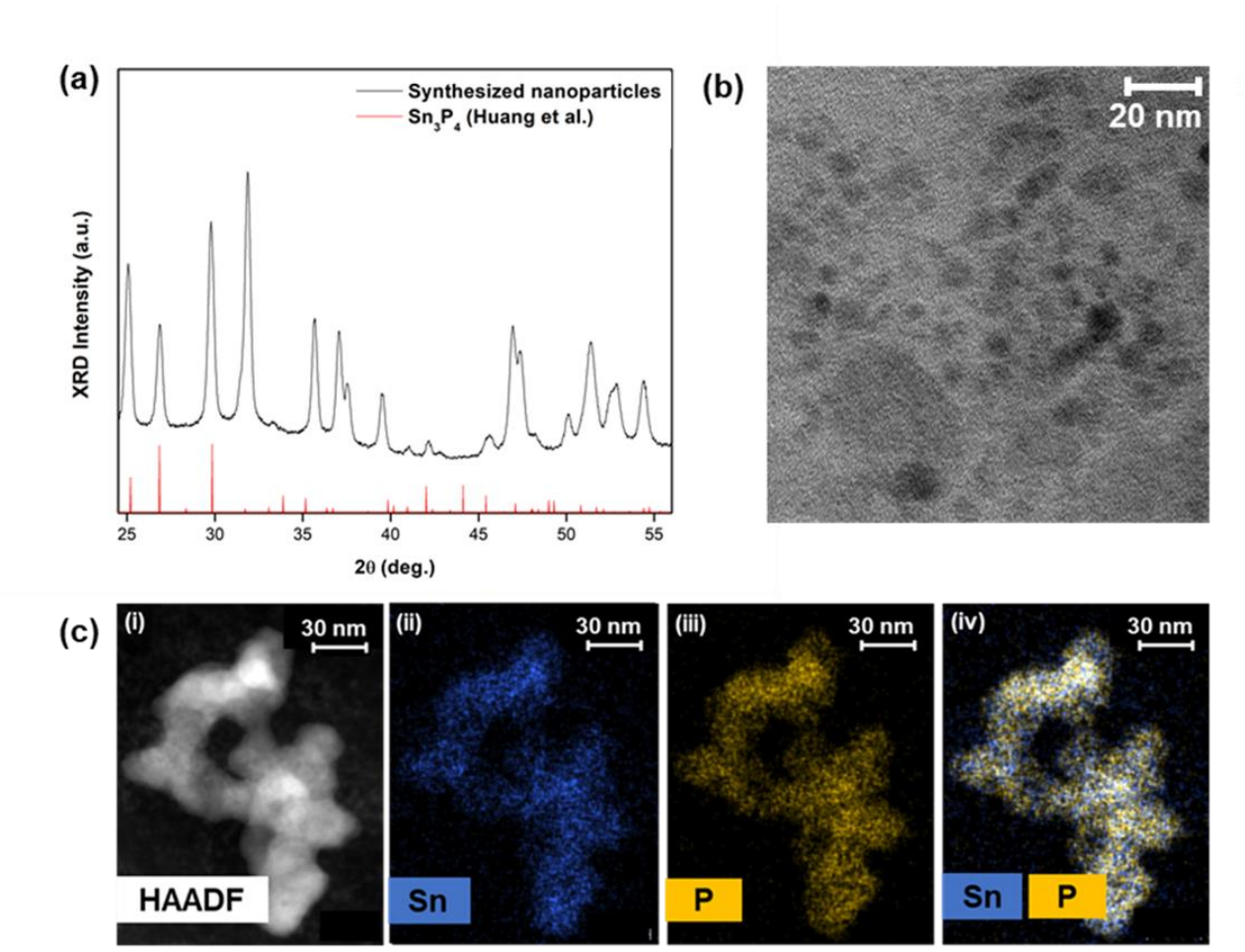

Figure S7. Phase and morphology of Sn_3P_4 nanocrystals. (**a**) X-ray diffraction data (XRD) obtained for Sn_3P_4 nanocrystals plotted against reference data for trigonal Sn_3P_4 provided by Huang *et al*.[4] (**b**) Bright field TEM images for synthesized nanocrystals. (**c**) Scanning transmission electron microscopy (STEM) images and energy dispersive X-ray (EDX) data for synthesized nanocrystals.

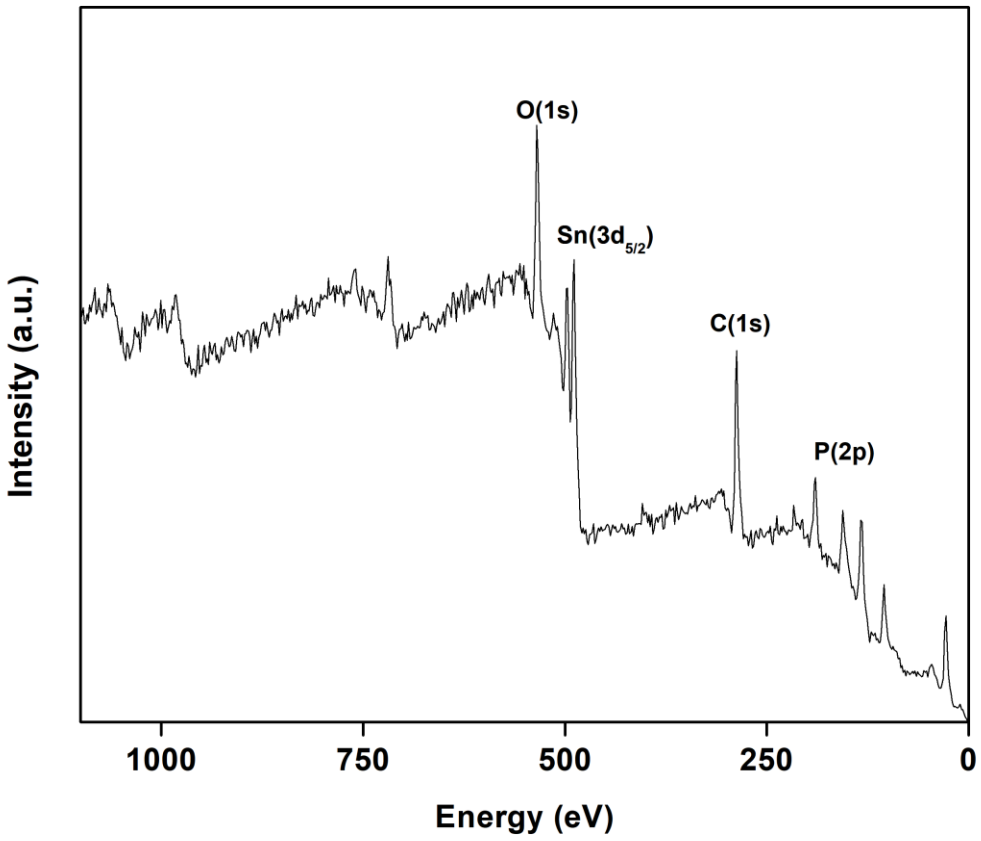

Figure S8. Survey data obtained for SnP measured using x-ray photoelectron spectroscopy (XPS).

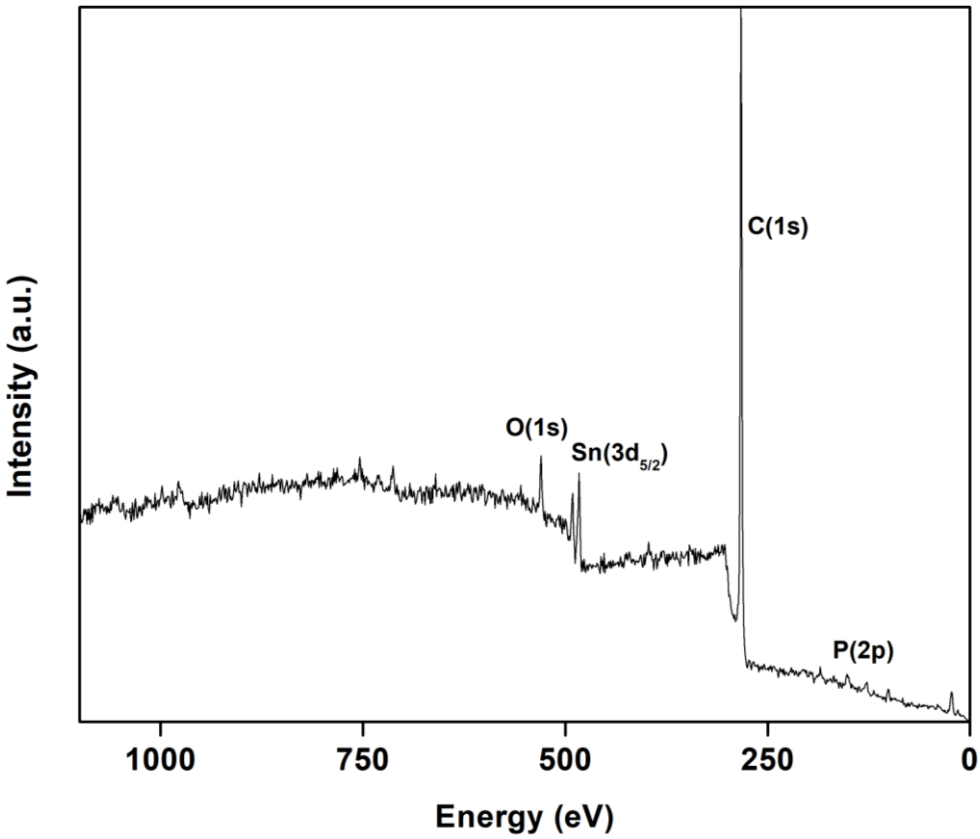

Figure S9. Survey data obtained for Sn_3P_4 measured using x-ray photoelectron spectroscopy (XPS).

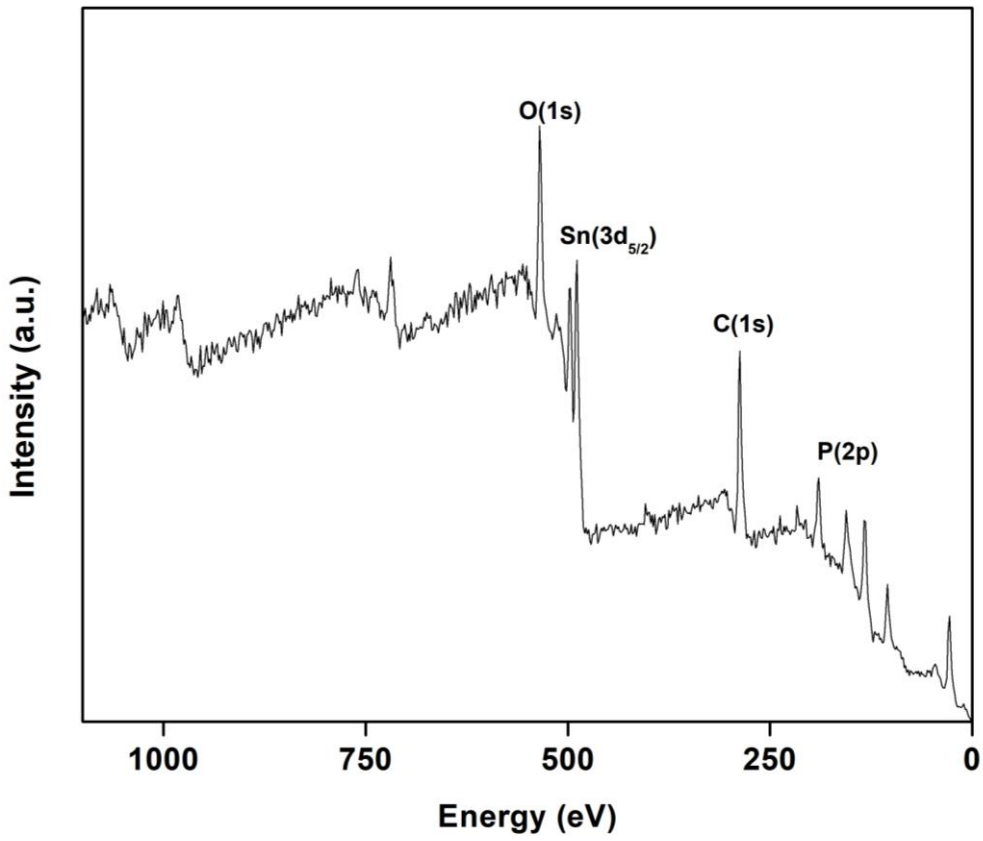

Figure S10. Survey data obtained for Sn_4P_3 measured using x-ray photoelectron spectroscopy (XPS).

Table S2. Best fit parameters obtained by EXAFS analysis of the k^2-weighted spectrum of the synthesized SnP. The experimental data was fit against trigonal SnP (ICSD-69026). R-factor as well as reduced χ_{red}^2 are included. SnP data were fit with an *r* range of 1.1 to 2.8 Å and *k* range of 2.0 to 9.0 $Å^{-1}$. Sn-O and Sn-P photoelectron paths were used in the fits.

Structure Model	Path	N	R(Å)	σ^2 (Å^2)	ΔE_0 (eV)	R(%)	χ_{red}^2	S_0^2
SnP (ICSD-69026)	Sn-O	0.7±0.4	2.02±0.18	0.0057±0.0068	7.5±0.5	0.4	11	1.1
	Sn-P	2.9±0.7	2.69 ± 0.13	0.012±0.0034				

1

Table S3. Influence of k weighting on the obtained coordination numbers *N* by EXAFS analysis of synthesized SnP. The experimental data was fit against trigonal SnP (ICSD-69026). SnP data were fit with an *r* range of 1.1 to 2.8 Å and k range of 2.0 to 9.0 $Å^{-1}$. Sn-O and Sn-P photoelectron paths were used in the fits.

Path	**N**	**k weighting**
Sn-O	0.7±0.5	k
Sn-P	2.6±0.8	
Sn-O	0.7±0.4	k^2
Sn-P	2.9±0.7	
Sn-O	1.0±0.6	k^3
Sn-P	2.7±0.6	
Sn-O	0.7±0.4	k, k^2
Sn-P	2.6±0.7	
Sn-O	0.8±0.4	k^2, k^3
Sn-P	2.7±0.6	
Sn-O	0.7±0.4	k, k^2, k^3
Sn-P	2.6±0.7	

Table S4. Best fit parameters obtained by EXAFS analysis of the k^2-weighted spectrum of the synthesized Sn_4P_3. The fit was performed using an Sn-P path for the rhombohedral phase of Sn_4P_3 (ICSD-15014). The fits were performed using a *k* range of 2.3 to 11.45 $Å^{-1}$ and an *r* range of 1.45 to 3 Å.

Structure Model	Path	N	R(Å)	σ^2 ($Å^2$)	ΔE_0 (eV)	R (%)	S_0^2	χ_{red}^2
Sn_4P_3 (ICSD-15014)	Sn-P	1.2±0.1	2.65±0.02	0.0085±0.0013	6.3±0.9	1.3	1.1	64

Table S5. Best fit parameters obtained by EXAFS analysis of the k^2-weighted spectrum of the synthesized Sn_3P_4. The fit was performed using the Sn-P path for tetragonal phase of SnP (ICSD-16077). R-factor as well as reduced χ^2 are included. The fits were performed using a *k* range of 2.5 to 10.5 $Å^{-1}$ and an *r* range of 1.1 to 2.7 Å.

Structure Model	Path	N	R(Å)	σ^2 ($Å^2$)	ΔE_0 (eV)	R(%)	S_0^2	χ_{red}^2
Sn_3P_4 (ICSD-16077)	Sn-O	0.3±0.3	2.03±0.19	0.0040±0.0084	8.2±1.4	1.5	1.1	13
	Sn-P	1.3±0.2	2.66±0.18	0.0054±0.0014				

References

1. B. H. Toby and R. B. Von Dreele, *J. Appl. Crystallogr.* **2013,** *46* (2), 544-549.
2. C. A. Schneider, W. S. Rasband, and K. W. Eliceiri, *Nat. Methods* **2012,** *9* (7), 671-675.
3. B. Ravel, M. Newville, *J. Synchrotron Rad.* **2005,** *12* (4), 537-541.
4. M. Huang and Y. P. Feng, *Phys. Rev. B*, 2004, **70**, 184116.